Physics and Chemistry of the Earth 100 (2017) 101–111

Contents lists available at ScienceDirect

Physics and Chemistry of the Earth

journal homepage: www.elsevier.com/locate/pce

Evaluating the performance of the newly-launched Landsat 8 sensor in detecting and mapping the spatial configuration of water hyacinth (*Eichhornia crassipes*) in inland lakes, Zimbabwe

Timothy Dube [a, *], Onisimo Mutanga [b], Mbulisi Sibanda [b], Victor Bangamwabo [b], Cletah Shoko [b]

[a] Department of Geography and Environmental Science, University of Limpopo, Private Bag X1106 Sovenga, 0727, Polokwane, South Africa
[b] Discipline of Geography, School of Agricultural, Earth and Environmental Sciences, University of KwaZulu-Natal, P/Bag X01, Scottsville, Pietermaritzburg 3209, South Africa

ARTICLE INFO

Article history:
Received 14 April 2016
Received in revised form
12 January 2017
Accepted 17 February 2017
Available online 21 February 2017

Keywords:
Low cost
Monitoring
Data-scarce regions
Remote sensing
Spatial spread
Traditional techniques
Water weeds

ABSTRACT

The remote sensing of freshwater resources is increasingly becoming important, due to increased patterns of water use and the current or projected impacts of climate change and the rapid invasion by lethal water weeds. This study therefore sought to explore the potential of the recently-launched Landsat 8 OLI/TIRS sensor in mapping invasive species in inland lakes. Specifically, the study compares the performance of the newly-launched Landsat 8 sensor, with more advanced sensor design and image acquisition approach to the traditional Landsat-7 ETM+ in detecting and mapping the water hyacinth (*Eichhornia crassipes*) invasive species across Lake Chivero, in Zimbabwe. The analysis of variance test was used to identify windows of spectral separability between water hyacinth and other land cover types. The results showed that portions of the visible (B3), NIR (B4), as well as the shortwave bands (Band 8, 9 and 10) of both Landsat 8 OLI and Landsat 7 ETM, exhibited windows of separability between water hyacinth and other land cover types. It was also observed that on the use of Landsat 8 OLI produced high overall classification accuracy of 72%, when compared Landsat 7 ETM, which yielded lower accuracy of 57%. Water hyacinth had optimal accuracies (*i.e.* 92%), when compared to other land cover types, based on Landsat 8 OLI data. However, when using Landsat 7 ETM data, classification accuracies of water hyacinth were relatively lower (*i.e.* 67%), when compared to other land cover types (*i.e.* water with accuracy of 100%). Spectral curves of the old, intermediate and the young water hyacinth in Lake Chivero based on: (a) Landsat 8 OLI, and (b) Landsat 7 ETM were derived. Overall, the findings of this study underscores the relevance of the new generation multispectral sensors in providing primary data-source required for mapping the spatial distribution, and even configuration of water weeds at lower or no cost over time and space.

1. Introduction

Remote sensing of freshwater resources is increasingly becoming important for their proper management, especially in the light of increased water consumption and the current or projected impacts of climate change on this precious resource (Cavalli et al., 2009; Dube et al., 2015). Of particular consideration is the monitoring of water quality, which is a fundamental component in freshwater resources management. Besides, monitoring the quality of freshwater resources, such as lakes and dams becomes critical for improving water quality, as well as its management. Moreover, it has been discovered that freshwater resources are facing significant threats from invasion by aquatic weeds (Giardino et al., 2015; Palmer et al., 2015), which are a biological pollution, with significant effects on water quality, aquatic life and the ability to alter nutrients cycling. These invaders have therefore considerable implications to the subsequent water use (*e.g.* agriculture and domestic purposes, etc). Aquatic weeds also cause substantial damages to the fishing and tourism industries (Shekede et al., 2008; Wilson et al., 2007), resulting in severe financial losses

* Corresponding author.
E-mail address: timothy.dube@ul.ac.za (T. Dube).

http://dx.doi.org/10.1016/j.pce.2017.02.015
1474-7065/

(Hestir et al., 2008; Parochetti et al., 2008). In this regard, the monitoring of aquatic weeds provides essential information for proper mitigation and control measures to conserve the quality of water and ensure the continual provision of goods and services.

Ground-based measurements provides the most direct and accurate distribution of aquatic weeds (Ritchie et al., 2003; Sands and Nambiar, 1984). However, these measurements are time-consuming, labour-intensive and spatially limited (Ritchie et al., 2003). This approach is therefore difficult to implement over a large geographic coverage or for time-series analysis and even change detection monitoring. The availability of satellite data therefore provides great potential for the spatial and temporal monitoring of aquatic weeds in a timely and cost-effective approach (Dube et al., 2014; Giardino et al., 2015; Hestir et al., 2008; Shekede et al., 2008). In addition, remote sensing data enables large scale monitoring of aquatic weeds, which is not possible when using the more expensive, labour-intensive and time consuming ground-based measurements (Bossard et al., 2000). The repeated coverage of satellite sensors provide data for long-term monitoring, which is crucial in identifying the success of controlling measures of aquatic weeds (Penatti et al., 2015). This becomes valuable for a wide range of applications, which include, but not limited to the spatial and temporal analysis of their distribution, modelling of their expansion and their potential environmental impacts, which is highly desirable for local communities, environmental management agencies and decision makers.

Although hyperspectral images have high accuracy in classifying aquatic weeds, their applicability, especially in resources constrained environments, like sub-Saharan Africa is very limited, due to their high acquisition cost and low spatial coverage (Andrew and Ustin, 2008; Cavalli et al., 2009; Dube et al., 2015; Hamada et al., 2007; Hestir et al., 2008; Pengra et al., 2007; Siciliano et al., 2008). On the other hand, low spatial resolution sensors, such as MODIS and AVHRR, are presumed to be too coarse for the monitoring of water resources. Their large spatial resolution and broad spectral bands are not sufficient enough for the discrimination and classification of invasive species within freshwater resources. This limitation presents the Landsat mission as a better alternative in monitoring aquatic vegetation in data poor catchments.

The previous Landsat series data have been useful in monitoring the earth surface characteristics, such as land cover change analysis (Estoque and Murayama, 2015; Ji et al., 2006; Shalaby and Tateishi, 2007; Yuan et al., 2005), vegetation biomass (Lu, 2005; Zheng et al., 2004) and water loss quantification (McCabe and Wood, 2006). The sensors have also been helpful in monitoring inland waters (Palmer et al., 2015) and mapping invasive species (Peterson, 2005). Recently, Dube et al. (2014) reported the potential of the Landsat TM in mapping the water hyacinth invasive species in Lake Mutirikwi in Zimbabwe. Unfortunately, since 2011the Landsat TM sensor is no longer operational; hence its successful application is becoming limited. Moreover, the use of the active ETM+ sensor is associated with challenges associated with its scan line error failure, which developed in 2003, resulting in a loss of 22% of data for each scene (Chander et al., 2009). Nevertheless, despite its defects, data from the ETM+ sensor has been used (*e.g.* Dube and Mutanga (2015a)), due to the lack of other readily available datasets with better spatial, spectral, temporal and radiometric resolutions. Consequently, the emergence of the Landsat 8 sensor provides a better alternative for improved monitoring of the earth surface.

The advanced Landsat 8 sensor presents a new dataset for the continuation of the Landsat mission. Despite having the same spatial and temporal scales, the Landsat 8 sensor delivers satellite images with improved spectral and radiometric sensor capabilities, when compared to its predecessors (Roy et al., 2014). These sensor characteristics are more likely to enhance the sensitivity of the Landsat 8 to earth features. For example, the Landsat 8 satellite is characterised by an enhanced signal-to-noise performance and 12-bit radiometric resolution, which is more likely to have a considerable impact on its performance in detecting surface features (Dube and Mutanga, 2015b; Roy et al., 2014). Landsat 8 sensor has also a refined Near Infrared (NIR) spectral band, which improves its sensitivity to vegetation structural features (Dube and Mutanga, 2015b; Estoque and Murayama, 2015). Furthermore, the sensor acquires images using a push-broom scanning design, which is capable of increasing the sensor's spectral recording abilities (Dube and Mutanga, 2015a; Yuan et al., 2005), unlike the ETM+, or the previous Landsat sensors, which uses the whisk-broom design.

These improved sensor characteristics of the Landsat 8 are hypothesized to present pronounced prospects for detecting the spread and spatial configuration of invasive water hyacinth weeds in freshwater resources. So far, Landsat 8 satellite data has demonstrated its strength in quantifying total evaporation, thermal remote sensing and vegetation mapping related applications (Dube and Mutanga, 2015c; Jimenez-Munoz et al., 2014; Montanaro et al., 2014; Rozenstein et al., 2014; Yuan et al., 2005). This study, therefore, aims to explore the potential of the recently-launched Landsat 8 OLI/TIRS (Operational Land Imager/Thermal Infrared Sensor) sensor in mapping invasive species in inland lakes. To achieve this, the study compares the performance of the newly-launched Landsat 8 sensor, with more advanced sensor design and image acquisition approach to the traditional Landsat-7 ETM+ in detecting and mapping the water hyacinth (*Eichhornia crassipes*) invasive species across Lake Chivero, in Zimbabwe.

2. Materials and methods

2.1. Study area description

The study was conducted for Lake Chivero (Fig. 1), formerly known as Lake McLlwaine. The Lake is located 35 km away from the city of Harare, covering an area of about 6100 ha. Lake Chivero is one of the major water sources for the city of Harare and its surroundings. The Lake has been invaded by the water hyacinth (*Eichhornia crassipes*) weed, which has been worsened by the continuous disposal of raw sewerage from the surrounding urban areas. This provides the required nutrients for the optimal growth of the invasive species. Considering the role of this lake in providing water to vast of populations, fishing industry, recreational area and tourism, monitoring of the water hyacinth weed provides critical information for effective control, possible eradication measures and proper management of the Lake, to ensure the continual provision of services.

2.2. Remotely sensed data

Two Landsat missions; the Landsat 8 OLI and ETM images were used to discriminate the water hyacinth invasive weed for Lake Chivero. Two cloudless images of the respective sensors, covering the study area, were all acquired during the same dry season. Landsat 8 and ETM + images have a spatial resolution of 30-m and 16-day revisit time. The images were freely obtained from the online Landsat series archive (http://glovis.usgs.gov/web-link). The archived dataset is managed and distributed by the NASA (National Aeronautics and Space Administration) through the United States Geological Survey (USGS) Global Visualization Viewer (GVV). All the Landsat images of interest were acquired from the USGS web link in digital number (DN) format. Consequently, all these images (Landsat 8 and ETM+7) had to be calibrated from DN to radiances before analysis was undertaken. We converted the ETM+7 to the Top-of-Atmosphere (TOA) spectral radiances and further to at-

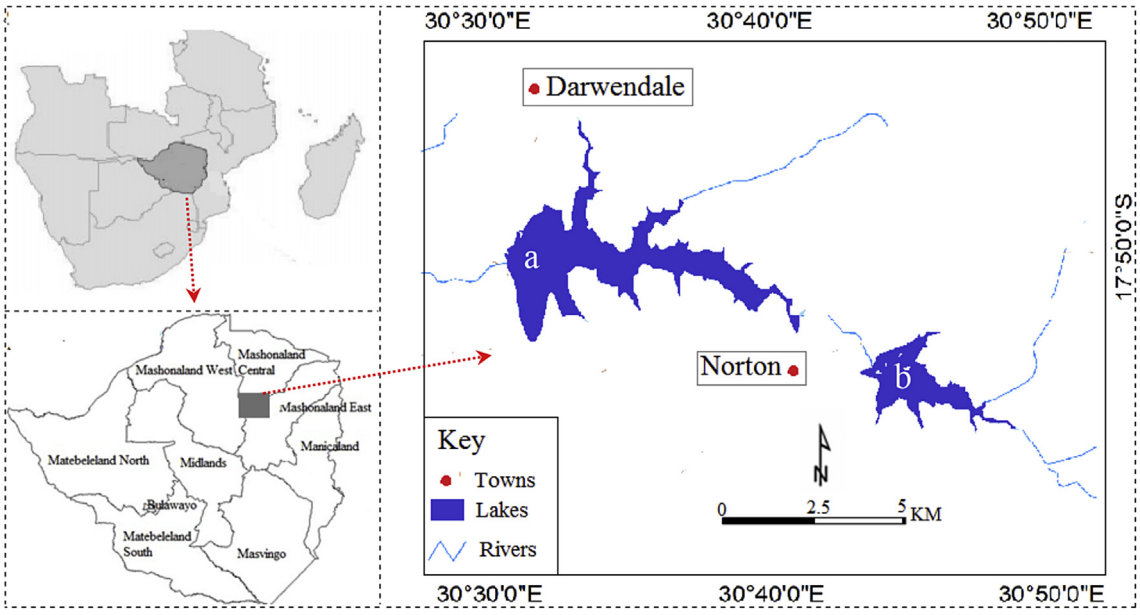

Fig. 1. Location of the study area (From the map *a* represents lake Manyame and b Chivero).

sensor spectral reflectances. The conversion was done as explained in literature, based on spectral reflectance rescaling constants (Ji et al., 2006). For the recently-launched Landsat 8 data, DN conversion to spectral reflectance was implemented in a GIS environment, using mathematical functions summarised on the USGS webpage (http://landsat.usgs.gov). All the images were then corrected for atmospheric effects (i.e. haze, non-target effects) using the Fast Line-of-sight Atmospheric Analysis of Spectral Hypercube radiative transfer model embedded in Envi software (Felde et al., 2003; Kaufman et al., 1997; Shalaby and Tateishi, 2007). Finally, the images were geometrically corrected using ground control points (GCPs).

2.3. Field surveys

For a comparative performance analysis of the two Landsat missions on discriminating inland Lakes management and monitoring we sought to discriminate water hyacinth from other land cover types, such as disturbed lands, woodlands, grasslands, plantations, bare land and water. We conducted a field survey on the 8th to the 13th of June 2015, to measure the locations of all the land cover types considered in this study, using a hand held Global Positioning System *e*-trex 10 (at ±5 m accuracy). Furthermore, three age groups of water hyacinth (old, intermediate and young) were identified; also their location measured using a GPS. A total of 274 points were utilised in discriminating water hyacinth from other land cover types. Meanwhile, 300 sample points were used to discriminate different age groups of hyacinth plants in the two lakes. The locations of each land cover type measured using a GPS were then imported into a geographic information system environment (ArcGIS 10.3 software) and converted into point maps (regions of interests) for classification purposes. The field survey was done at time that coincided with satellite overpass period. The point map was then overlaid on the pre-processed Landsat ETM+ 7 and 8 OLI acquired on the 6th and 12th of June 2015 respectively. Pre-processing was done to derive reflectances of each land cover type at each point across all the sections of the electromagnetic spectrum covered by the two images. The data was then exported as a table. Before conducting the classification process, the derived spectral reflectance datasets were then exported into Microsoft excel as a table. The data was then randomly split into a 70% for training and 30% testing samples.

2.4. Satellite data classification

2.4.1. Analysis of variance tests

The analysis of variance (ANOVA) test were used to identify (statistically significant ($\alpha = 0.05$)) windows of spectral separability between water hyacinth and other land cover types, as well as between the three different water hyacinth age groups based on both Landsat 8 OLI and 7 ETM wave bands. To establish the influence of each band in discriminating water hyacinth from other land cover types, discriminant analyses (DA), as well as variable importance scores were used in this study.

2.4.2. Image classification

To evaluate the robustness of the newly launched Landsat 8 data in discriminating water hyacinth, as well as differentiate different age groups of hyacinth, when compared to Landsat 7 ETM satellite data we used discriminant analysis (DA). In simple terms discriminant analysis was used to classify water hyacinth from other land cover types, as well as to classify different hyacinth age groups in XLSTAT 2013 version. DA seeks for linear combinations which optimally classifies each land cover types or hyacinth age groups (Sibanda et al., 2015). DA converts radiances data derived from satellite images into several components that influence the variations in radiance data amongst the land cover types (Sibanda et al., 2015). DA utilised a discriminant function to distinguish land cover types into classes based on a measure of generalized squared distances. Within-group covariance matrices were derived categorising all the samples into clusters which they had least generalised squared distances to producing classification and cross-validates results. In this study we used a stepwise (backward feature) method to discriminate different land cover types producing Eigen values. The Eigen values indicated how good certain wavebands classified different land cover types. Specifically, wave bands that retained larger Eigen values were recognised as the most influential in discriminating land cover types in this study (Sibanda et al.,

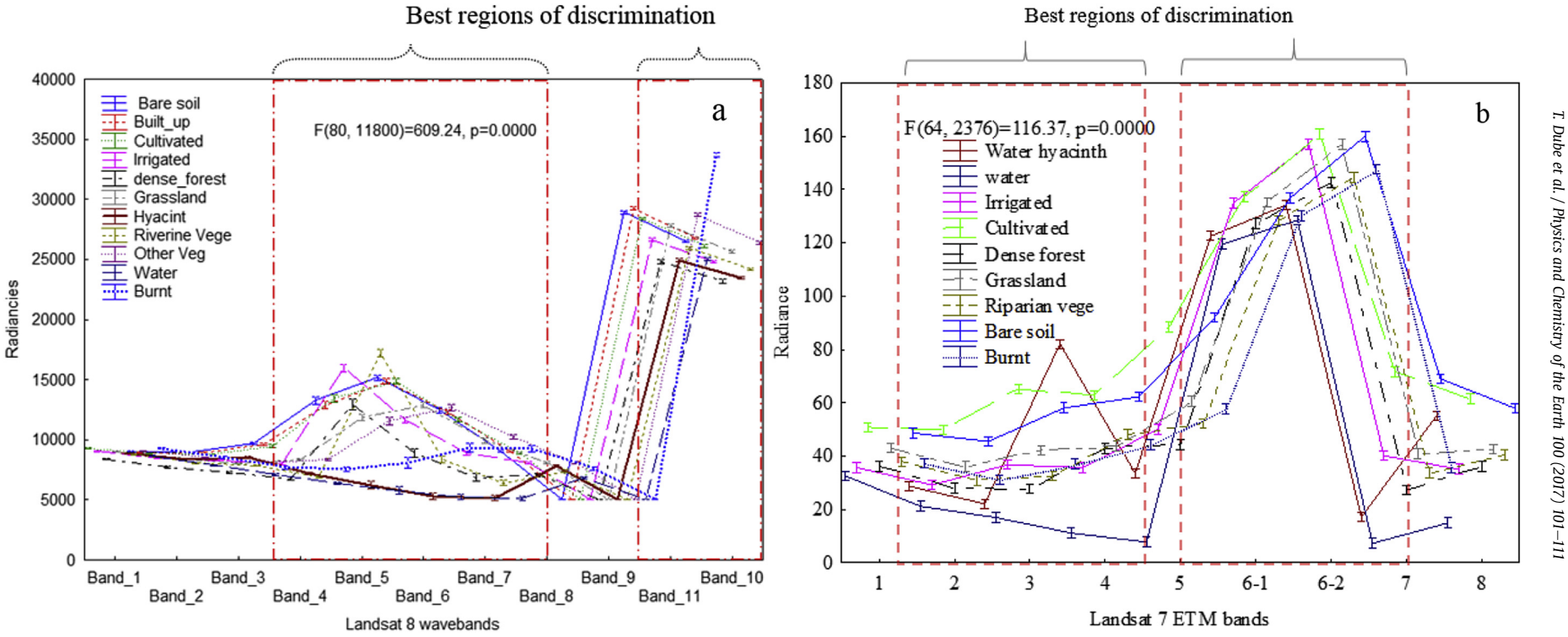

Fig. 2. Regions of spectral separability between water hyacinth and other and cover types using (a) Landsat 8 OLI and (b) Landsat 7 ETM remotely sensed data based on ANOVA.

Table 1
Confusion matrix derived from the dry season Landsat 8 image's 10 bands combination.

	Bare soil	Built up	Burnt areas	Cultivation	Cultivation Irri.	Grassland	Hyacinth	Other veg.	Riparian veg.	Water	Total	% correct
Bare soil	19	5	1	17	0	1	0	1	0	0	44	43.18%
Built up	3	35	0	2	1	0	0	5	1	0	47	74.47%
Burnt areas	0	0	37	0	0	0	0	1	0	0	38	97.37%
Cultivation	12	3	0	28	0	0	0	0	0	0	43	65.12%
Cultivation- Irrig.	0	0	0	0	34	0	0	0	9	0	43	79.07%
Grassland	0	0	0	2	2	38	0	1	0	1	44	86.36%
Hyacinth	0	0	0	0	3	0	44	0	0	1	48	91.67%
Other veg.	0	5	13	1	0	16	0	9	0	0	44	20.45%
Riperian veg.	0	0	0	0	7	0	4	0	28	5	44	63.64%
Water	0	0	0	0	0	0	1	0	0	40	41	97.56%
Total	34	48	51	50	47	55	49	17	38	47	436	71.56%

Table 2
Confusion matrix derived from the dry season Landsat 7 ETM+'s 9 bands combination.

from\to	Bare soil	Built up	Burnt	Grasslands	Hyacinth	Riparian veg.	Water	dense forest	dry fields	irrigated fields	Total	% correct
Bare soil	18	0	3	0	0	0	0	0	22	0	43	2
Built up	0	25	10	0	0	0	0	0	0	0	35	71
Burnt	11	0	24	7	0	0	4	0	0	0	46	52
Grasslands	0	0	0	28	0	0	0	0	0	9	37	76
Hyacinth	0	0	0	0	33	0	16	0	0	0	49	67
Riparian veg.	0	17	3	0	16	22	0	18	0	7	83	27
Water	0	0	0	0	0	0	24	0	0	0	24	100
dense forest	0	0	0	0	0	9	0	24	0	0	33	73
dry fields	14	0	0	5	0	0	0	0	24	0	43	56
irrigated fields	0	0	12	0	0	6	0	0	0	25	43	58
Total	**43**	**42**	**52**	**40**	**49**	**37**	**44**	**42**	**46**	**41**	**436**	**57**

Table 3
Confusion matrix obtained in classifying water hyacinth age groups based on Landsat 8 OLI.

	Intermediate	Old	Young	Total	% correct
Intermediate	67	9	4	80	84
Old	2	38	0	40	95
Young	0	0	41	41	100
Total	**69**	**47**	**45**	**161**	**91**

2015). We then tested whether the within covariance matrices were equal based on the Box test (Fisher's F asymptotic approximation), Mahalanobis distances, Wilks' Lambda test (Rao's approximation), and Kullback's test (Sibanda et al., 2015). All these tests indicated that there were significant differences ($\alpha = 0.05$) amongst covariance matrices of each land cover type. All the above computations were conducted to derive a mathematical model for classifying hyacinth from other land covers types as well as classifying different hyacinth plant age groups. The derived models were then used to map different land cover types including hyacinth and its different age groups based on raster calculator in ArcGIS 10.3 software.

2.5. Remote sensing image classification accuracy

Image classification accuracy results obtained from the discriminant analysis classification ensemble were generated based on the recent Pontius and Millones' quantity agreement and disagreement allocations technique. Information on the quantity disagreement is obtained through the summation of differences between the training and model validation datasets (Adelabu and Dube, 2014; Sibanda et al., 2015). On the other hand, model agreement between the testing (30%) and training (70%) data was derived through subtracting the two disagreements from 100%. The allocations of agreement, omission disagreement, and commission disagreement for DA classification ensemble were derived from the confusion matrix as proposed by Pontius and Millones. Based on the derived confusion matrix we then calculated the overall, user and producer accuracies. Finally, the classification performances of Landsat 8 OLI and Landsat 7 ETM satellite data was then assessed using the McNemar test (de Leeuw et al., 2006) with $\alpha = 0.05$.

3. Results

3.1. Discriminating water hyacinth from other land cover types

Following the analysis of variance tests, it can be observed that portions of the visible (Bands 3), NIR (Band 4) as well as the shortwave bands (Band 8, 9 and 10) of both Landsat 8 OLI and Landsat 7 ETM, exhibited windows of separability between water hyacinth and other land cover types (Fig. 2 a). However, Landsat 7 OLI wavebands 1, 2 and 9 there were no significant differences between water hyacinth and other land cover types. Comparatively, Landsat 8 & ETM bands 1 and 8 did not yield any significant differences between water hyacinth and other land cover types (Fig. 2 b) (Table 1).

Tables 2 and 3 illustrate the classification accuracies derived from classifying water hyacinth using Landsat 8 OLI and Landsat 7 ETM satellite data, respectively. It was observed that based on Landsat 8 OLI, an overall classification accuracy of 72% was achieved, when compared Landsat 7 ETM, which yielded an accuracy of 57%. Water hyacinth had optimal accuracies (*i.e.* 92%), when compared to other land cover types, based on Landsat 8 OLI data. However, when using Landsat 7 ETM data, classification accuracies of water hyacinth were relatively lower (*i.e.* 67%), when compared to other land cover types (*i.e.* water with accuracy of 100%).

Fig. 3 illustrates the classification accuracies across all land cover types based on Landsat (a) 8 OLI and (b) 7 ETM satellite data. It can

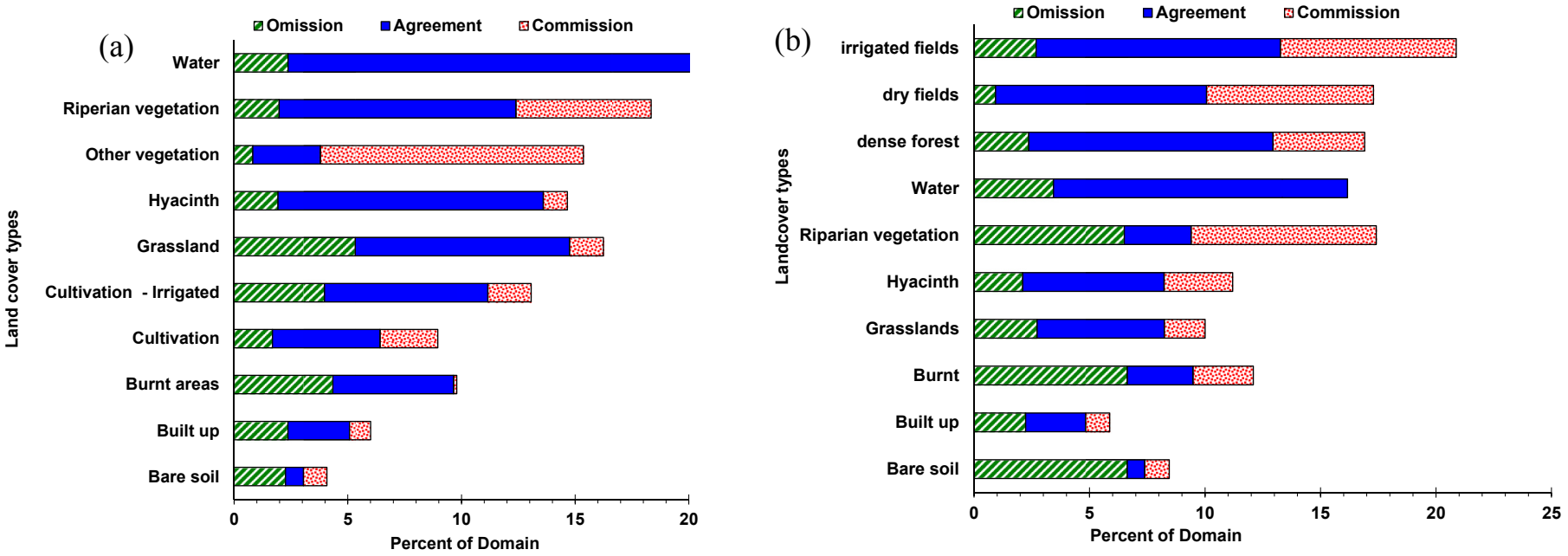

Fig. 3. Classification accuracies based on (a) Landsat 8 and (b) Landsat 7 satellite data.

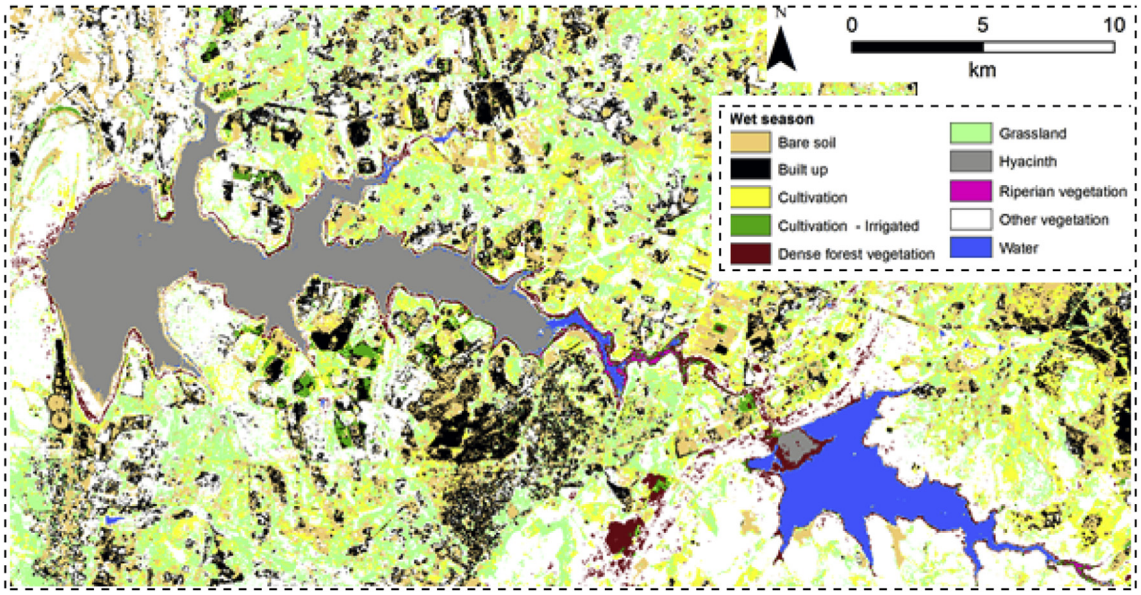

Fig. 4. Land cover types derived using Landsat 8 satellite data.

be observed that when using Landsat 8 OLI data, the allocations of commission and omission are lower for water hyacinth when compared to classification based on Landsat 7 ETM satellite data. It can be observed that when using both Landsat 8 OLI and Landsat 7 ETM all land cover types had relatively higher allocations of commission and omission, when compared to the water hyacinth class. Fig. 4 shows the spatial distribution of all land cover types around the Lake Chivero based on the classification of Landsat 8 OLI satellite data.

3.2. Classification of different water hyacinth age groups

Fig. 5 shows the spectral curves of the old, intermediate and the young water hyacinth in Lake Chivero based on: (a) Landsat 8 OLI, and (b) Landsat 7 ETM. It can be observed from Fig. 5 (a) that the wavebands that exhibited spectral separability windows in discriminating young, intermediate and old water hyacinth in Lake Chivero were based on Landsat 8 OLI bands 8, 9 and 10. When using Landsat 7 ETM bands 4, 5, 6-2, 7 and 8 yielded windows of spectral separability amongst the young, intermediate and old water hyacinth in Lake Chivero.

Fig. 6 illustrates the classification accuracies of discriminating young intermediate and old water hyacinth plants in Lake Chivero. Landsat 8 performed better than Landsat 7 considering the higher magnitudes in terms of the allocation of agreement than allocations of disagreement (allocations of omission and commission). Landsat 7 ETM satellite data yielded relatively higher allocation of disagreement. Considering the optimal classification accuracies derived based on Landsat 8 OLI, Fig. 7 portrays the spatial distribution of the three water hyacinth age groups. The young aged water hyacinth occupied a relatively smaller spatial extent, with the older age group occupying the biggest spatial extent.

Tables 3 and 4 presents classification accuracy details of each water hyacinth age group based on (a) Landsat 8 OLI and (b) Landsat 7 ETM. Landsat 7 ETM satellite data yielded a lower overall classification accuracy of 67% when compared to Landsat 8 OLI satellite data which resulted in an overall classification accuracy of 91%. When assessing the classification accuracy of each class, the young aged water hyacinth plants had better accuracies when compared to both the intermediate and old water hyacinth plants in Lake Chivero.

4. Discussion

The main aim of this research was to test the feasibility of using the new generation Landsat 8 sensor, compared to its predecessor, the Landsat ETM+7, in detecting, classifying and mapping the water hyacinth invasive species in Lake Chivero, Zimbabwe. This information is fundamental for well-informed management of water resources, especially in water-scarce environments of sub-Saharan Africa. Above all, the reliable distribution and extent of the water hyacinth are required to determine its severity through time, relate its abundance to environmental factors (*e.g.* climate change), identify threatened water resources for the provision of control measures, as well as to assess their effectiveness.

Findings from this study have shown the capability of the new generation Landsat 8 multispectral sensor in mapping the water hyacinth species, with reasonable accuracy, when compared to Landsat ETM+. For instance, using the Landsat 8 OLI, an overall classification accuracy of 72% was achieved, compared to the 57% derived based on the Landsat 7 ETM data. This shows that the Landsat 8 sensor has better water hyacinth discrimination abilities which enhance its classification accuracy. The better performance of Landsat 8 in detecting the water hyacinth maybe be attributed to its unique and advanced sensor design, when compared to the Landsat ETM+. The recent study by Pahlevan and Schott (2013) has reported the potential of the Landsat 8 sensor in monitoring coastal/inland water resources with accuracies not achievable using its predecessors. They further pointed out that the Landsat 8 sensor acquisition approach, which is characterized by band-specific detectors, increases its ability to provide a detailed scan of the surface. In addition, the Landsat 8 sensor images the surface using 'along track' approach which boosts its sensitivity to the most critical biophysical characteristics of vegetation (Dube and Mutanga, 2015a). Better performance of the Landsat 8 sensor was also observed in water hyacinth species detection accuracy, where an optimal accuracy of 92% was yielded, when compared to other land cover types. On the contrary, the Landsat 7 ETM+ data produced relatively lower water hyacinth (*i.e.* 67%) classification accuracies, when compared to other land cover types (*i.e.* water with accuracy

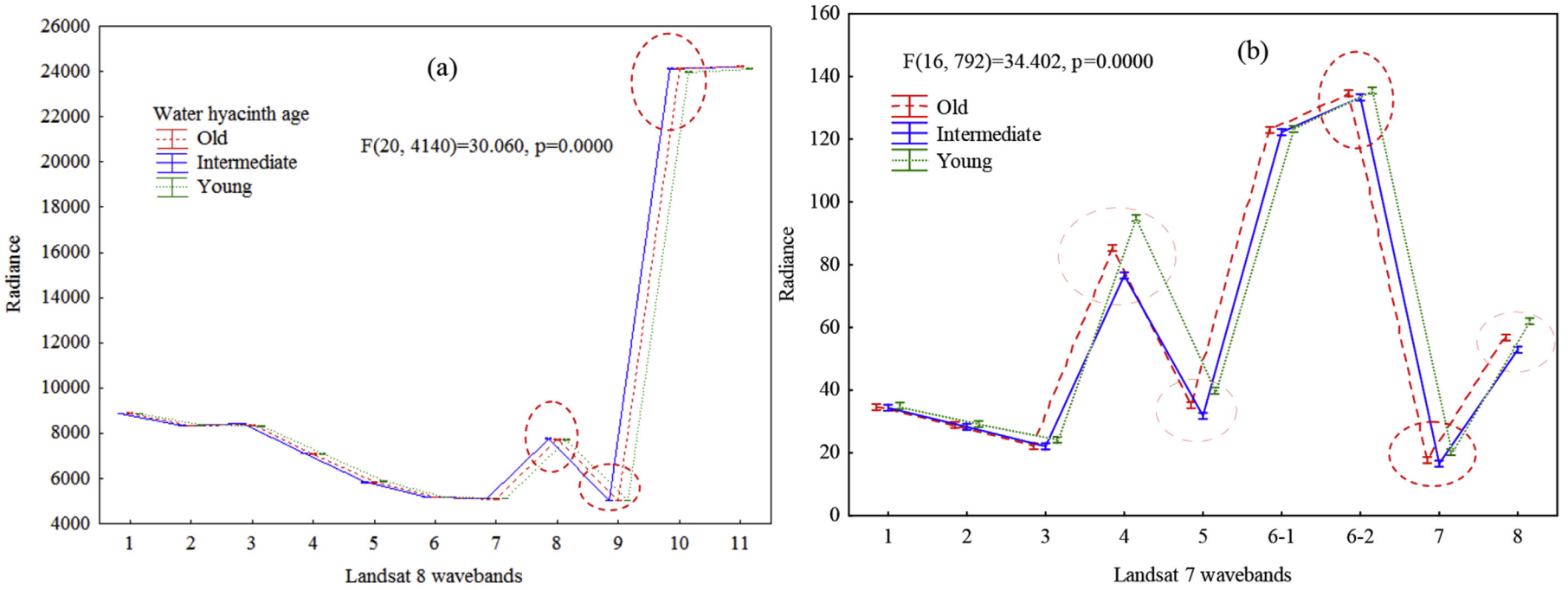

Fig. 5. The spectral characteristics of young, intermediate and old water hyacinth age groups derived, using the new Landsat 8 data. Letters denote bands that exhibit significant ($\alpha = 0.05$) differences amongst the water hyacinth age groups.

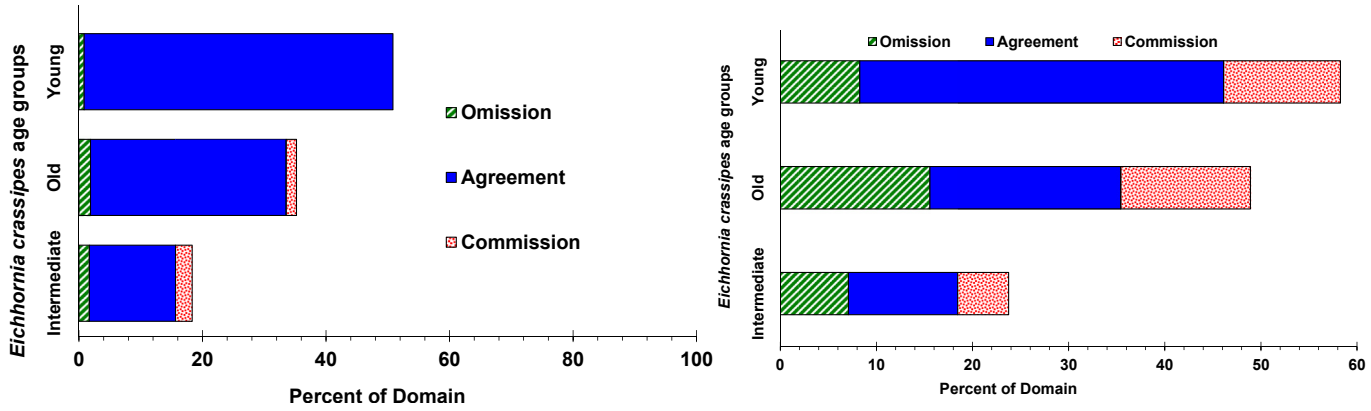

Fig. 6. Water hyacinth classification accuracies derived based on (a) Landsat 8 OLI and (b) Landsat 7 ETM satellite data.

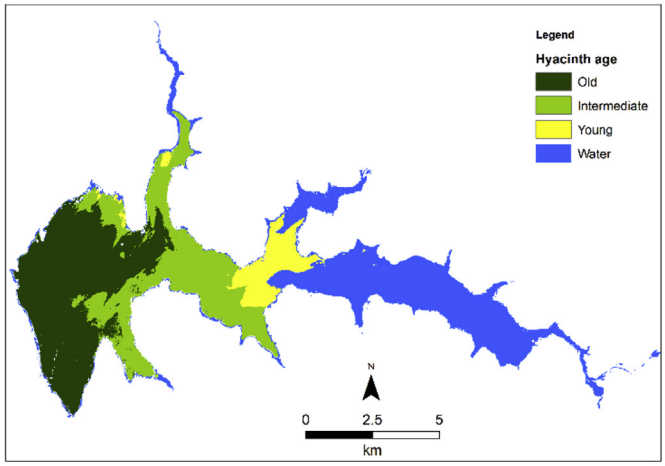

Fig. 7. Spatial distribution of different water hyacinth.

Table 4
Confusion matrix obtained in classifying water hyacinth age groups based on Landsat 7 ETM.

from\to	Intermediate	Old	Young	Total	% correct
Intermediate	30	9	5	44	68
Old	10	28	9	47	60
Young	0	9	28	37	76
Total	**40**	**46**	**42**	**128**	**67**

of 100%). The lower classification from the Landsat ETM+ may be attributed to a number of factors. For instance, the sensor operates using the whisky-broom approach, with limited dwell-time on the target. In addition, its 8-bit radiometric resolution reduces its ability to discriminate different vegetation characteristics, resulting in low sensitivity to critical species properties. The lower accuracy of the Landsat ETM+ has also been noted by El-Askary et al. (2014), they highlighted that it is likely attributed to the weak signal-to-noise ratio of the ETM+ 7 sensor, which reduces the accurate retrieval of species reflectance, thereby reducing the classification accuracy. Furthermore, the lower classification ability of the Landsat ETM+ 7 may also emanate from the failure of the Scan Line Corrector, which result in a loss of approximately 22% of data for each image scene (Chander et al., 2009).

4.1. Classification of different water hyacinth plants age groups

The Landsat 8 sensor has also confirmed its improved discrimination ability in detecting the different age groups of the water hyacinth species. The sensor was thus able to differentiate and classify the different species age groups, when compared to Landsat ETM+ 7. This may be due to the presence of the refined near-infrared spectral band that plays a fundamental role in enhancing the spectral response of the different age groups, using the Landsat 8 data. Moreover, the study by Jia et al. (2014) has noted that the refined near-infrared band inhibits the absorption of water vapour, thereby reducing sensor spectral saturation challenges and allowing the accurate retrieval of species spectral signatures. The enhanced 12-bit radiometric resolution further enables the sensor to accurately detect and discern the different water hyacinth species age groups. On the contrary, the long serving Landsat ETM+ 7 sensor constitute a broad near infrared spectral band, which has low detection ability and hence fails to discriminate the different species age groups. This has been discovered by previous studies, which highlighted that the broad near-infrared band of the Landsat ETM+ 7 results in the absorption effect of water vapour, thereby limiting the accurate acquisition of surface reflectance (Dube and Mutanga, 2015a; Irons et al., 2012; Jia et al., 2014). They further noted that the shorter dwelling-time on the target of the sensor is hypothesized to reduce its radiometric resolution. This results in the reduction of the spectral record precision which introduces saturation challenges.

The findings of this study prove the potential of the advanced Landsat 8 push-broom sensor in discriminating and mapping the water hyacinth, when compared to the Landsat ETM+ 7. The Landsat 8 thus presents a new advanced dataset for large-scale monitoring of invasive species critical in the conservation of freshwater resources, especially considering the defects of the active ETM+ 7 sensor, as well as the low accuracy and decommissioning of the other TM sensors (Pahlevan and Schott, 2013; Palmer et al., 2015). Based on the findings of this study, the Landsat 8 multispectral sensor presents an attractive dataset for large-scale mapping of the water hyacinth invasive species, with plausible estimates, when compared to the ETM+ 7 sensor, especially in resource-constrained areas. Moreover, the readily availability of the Landsat 8 poses an invaluable opportunity for large-scale monitoring, especially considering the challenges faced with the use of high resolution hyperspectral, radar and lidar sensors, which are very expensive, spatially limited, and face saturation problems (Dube and Mutanga, 2015a, b). Thus, the use of images with high classification accuracies, such as hyperspectral in mapping water hyacinth remains a challenge.

Although the use of the Landsat ETM + data produced lower classification accuracy for the water hyacinth invasive species, when compared to the use of Landsat 8, previous studies have identified the feasibility of the former in other studies, such as forest biomass (Cohen et al., 2003; Lu, 2005) with reasonable accuracy. Furthermore, the Landsat ETM sensor remains applicable in earth imaging at landscape levels, such as fields at which the area is not affected by the scale line error.

5. Conclusion

The present study compared the potential of the new generation Landsat 8 and the long-serving ETM+ sensors in classifying and mapping the water hyacinth invasive species in Lake Chivero, freshwater resource, in Zimbabwe. The findings from this study have proved that the more advanced Landsat 8 multispectral sensor presents a valuable data-source for the accurate mapping of invasive species, in resource-constrained regions of sub-Saharan Africa, compared to the ETM + sensor. The strength of the newly-launched pushbroom Landsat 8 sensor however, needs to be further examined in natural environments with heterogeneous forests where the amount of biomass is highly variable. The results of this work however provide the necessary insight and motivation to the remote sensing community; ecologists and environmentalists to shifting toward identifying the most suitable, cheap and readily available remote sensing sensors necessary for reliable and accurate aboveground forest biomass monitoring especially in data-scarce environments.

Acknowledgements

The authors are grateful to the National Aeronautics and Space Administration for the provision of remote sensing data and to anonymous reviewers for their valuable comments.

References

Adelabu, S., Dube, T., 2014. Employing ground and satellite-based QuickBird data and random forest to discriminate five tree species in a Southern African Woodland. Geocarto Int. 30, 457–471.
Andrew, M.E., Ustin, S.L., 2008. The role of environmental context in mapping invasive plants with hyperspectral image data. Remote Sens. Environ. 112, 4301–4317.
Bossard, C.C., Randall, J.M., Hoshovsky, M.C., 2000. Invasive Plants of California's Wildlands. Univ of California Press.
Cavalli, R.M., Laneve, G., Fusilli, L., Pignatti, S., Santini, F., 2009. Remote sensing water observation for supporting lake Victoria weed management. J. Environ. Manag. 90, 2199–2211.
Chander, G., Markham, B.L., Helder, D.L., 2009. Summary of current radiometric calibration coefficients for Landsat MSS, TM, ETM+, and EO-1 ALI sensors. Remote Sens. Environ. 113, 893–903.
Cohen, W.B., Maiersperger, T.K., Gower, S.T., Turner, D.P., 2003. An improved strategy for regression of biophysical variables and Landsat ETM+ data. Remote Sens. Environ. 84, 561–571.
de Leeuw, J., Jia, H., Yang, L., Liu, X., Schmidt, K., Skidmore, A.K., 2006. Comparing accuracy assessments to infer superiority of image classification methods. Int. J. Remote Sens. 27, 223–232.
Dube, T., Gumindoga, W., Chawira, M., 2014. Detection of land cover changes around Lake Mutirikwi, Zimbabwe, based on traditional remote sensing image classification techniques. Afr. J. Aquatic Sci. 39, 89–95.
Dube, T., Mutanga, O., 2015a. Evaluating the utility of the medium-spatial resolution Landsat 8 multispectral sensor in quantifying aboveground biomass in uMgeni catchment, South Africa. ISPRS J. Photogramm. Remote Sens. 101, 36–46.
Dube, T., Mutanga, O., 2015b. Investigating the robustness of the new Landsat-8 Operational Land Imager derived texture metrics in estimating plantation forest aboveground biomass in resource constrained areas. ISPRS J. Photogramm. Remote Sens. 108, 12–32.
Dube, T., Mutanga, O., 2015c. Quantifying the variability and allocation patterns of aboveground carbon stocks across plantation forest types, structural attributes and age in sub-tropical coastal region of KwaZulu Natal, South Africa using remote sensing. Appl. Geogr. 64, 55–65.
Dube, T., Mutanga, O., Seutloali, K., Adelabu, S., Shoko, C., 2015. Water quality monitoring in sub-Saharan African lakes: a review of remote sensing applications. Afr. J. Aquatic Sci. 40, 1–7.
El-Askary, H., Abd El-Mawla, S., Li, J., El-Hattab, M., El-Raey, M., 2014. Change detection of coral reef habitat using Landsat-5 TM, Landsat 7 ETM+ and Landsat 8 OLI data in the red sea (Hurghada, Egypt). Int. J. Remote Sens. 35, 2327–2346.
Estoque, R.C., Murayama, Y., 2015. Classification and change detection of built-up lands from Landsat-7 ETM+ and Landsat-8 OLI/TIRS imageries: a comparative assessment of various spectral indices. Ecol. Indic. 56, 205–217.
Felde, G.W., Anderson, G.P., Cooley, T.W., Matthew, M.W., Adler-Golden, S.M., Berk, A., Lee, J., 2003. Analysis of Hyperion data with the FLAASH atmospheric correction algorithm. In: Geoscience and Remote Sensing Symposium, 2003. IGARSS'03. Proceedings. 2003 IEEE International. IEEE, pp. 90–92.
Giardino, C., Bresciani, M., Valentini, E., Gasperini, L., Bolpagni, R., Brando, V.E., 2015. Airborne hyperspectral data to assess suspended particulate matter and aquatic vegetation in a shallow and turbid lake. Remote Sens. Environ. 157, 48–57.
Hamada, Y., Stow, D.A., Coulter, L.L., Jafolla, J.C., Hendricks, L.W., 2007. Detecting Tamarisk species (Tamarix spp.) in riparian habitats of Southern California using high spatial resolution hyperspectral imagery. Remote Sens. Environ. 109, 237–248.
Hestir, E.L., Khanna, S., Andrew, M.E., Santos, M.J., Viers, J.H., Greenberg, J.A., Rajapakse, S.S., Ustin, S.L., 2008. Identification of invasive vegetation using hyperspectral remote sensing in the California delta ecosystem. Remote Sens. Environ. 112, 4034–4047.
Irons, J.R., Dwyer, J.L., Barsi, J.A., 2012. The next Landsat satellite: the Landsat data continuity mission. Remote Sens. Environ. 122, 11–21.
Ji, W., Ma, J., Twibell, R.W., Underhill, K., 2006. Characterizing urban sprawl using multi-stage remote sensing images and landscape metrics. Comput. Environ. Urban Syst. 30, 861–879.
Jia, K., Wei, X., Gu, X., Yao, Y., Xie, X., Li, B., 2014. Land cover classification using Landsat 8 operational land imager data in Beijing, China. Geocarto Int. 29, 941–951.
Jimenez-Munoz, J.C., Sobrino, J., Skokovic, D., Mattar, C., Cristobal, J., 2014. Land surface temperature retrieval methods from Landsat-8 thermal infrared sensor data. geoscience and remote sensing letters. IEEE 11, 1840–1843.
Kaufman, Y.J., Wald, A.E., Remer, L., Gao, B.-C., Li, R.-R., Flynn, L., 1997. The MODIS 2.1-μm channel-correlation with visible reflectance for use in remote sensing of aerosol. Geosci. Remote Sens. IEEE Trans. 35, 1286–1298.
Lu, D., 2005. Aboveground biomass estimation using Landsat TM data in the Brazilian Amazon. Int. J. Remote Sens. 26, 2509–2525.
McCabe, M.F., Wood, E.F., 2006. Scale influences on the remote estimation of evapotranspiration using multiple satellite sensors. Remote Sens. Environ. 105, 271–285.
Montanaro, M., Gerace, A., Lunsford, A., Reuter, D., 2014. Stray light artifacts in imagery from the Landsat 8 thermal infrared sensor. Remote Sens. 6, 10435–10456.
Pahlevan, N., Schott, J.R., 2013. Leveraging EO-1 to evaluate capability of new generation of Landsat sensors for coastal/inland water studies. Sel. Top. Appl. Earth Obs. Remote Sens. IEEE J. 6, 360–374.
Palmer, S.C., Kutser, T., Hunter, P.D., 2015. Remote sensing of inland waters: challenges, progress and future directions. Remote Sens. Environ. 157, 1–8.
Parochetti, J., Arsenovic, M., Getsinger, K., Stubbs, D., Haller, W., 2008. Herbicides for Aquatic Weeds: Addressing the Need for Herbicides for Aquatic Weeds in Irrigation Water in the US. Out looks on Pest Management.
Penatti, N.C., Almeida, T.I.R.d., Ferreira, L.G., Arantes, A.E., Coe, M.T., 2015. Satellite-based hydrological dynamics of the world's largest continuous wetland. Remote Sens. Environ. 170, 1–13.
Pengra, B.W., Johnston, C.A., Loveland, T.R., 2007. Mapping an invasive plant, Phragmites australis, in coastal wetlands using the EO-1 Hyperion hyperspectral sensor. Remote Sens. Environ. 108, 74–81.
Peterson, E., 2005. Estimating cover of an invasive grass (Bromus tectorum) using tobit regression and phenology derived from two dates of Landsat ETM+ data. Int. J. Remote Sens. 26, 2491–2507.
Ritchie, J.C., Zimba, P.V., Everitt, J.H., 2003. Remote sensing techniques to assess water quality. Photogramm. Eng. Remote Sens. 69, 695–704.
Roy, D.P., Wulder, M.A., Loveland, T.R., C.E, W., Allen, R.G., Anderson, M.C., Helder, D., Irons, J.R., Johnson, D.M., Kennedy, R., Scambos, T.A., Schaaf, C.B., Schott, J.R., Sheng, Y., Vermote, E.F., Belward, A.S., Bindschadler, R., Cohen, W.B., Gao, F., Hipple, J.D., Hostert, P., Huntington, J., Justice, C.O., Kilic, A., Kovalskyy, V., Lee, Z.P., Lymburner, L., Masek, J.G., McCorkel, J., Shuai, Y., Trezza, R., Vogelmann, J., Wynne, R.H., Zhu, Z., 2014. Landsat-8: science and product vision for terrestrial global change research. Remote Sens. Environ. 145, 154–172.
Rozenstein, O., Qin, Z., Derimian, Y., Karnieli, A., 2014. Derivation of land surface temperature for Landsat-8 TIRS using a split window algorithm. Sensors 14, 5768–5780.
Sands, R., Nambiar, E.S., 1984. Water relations of pinus radiata in competition with weeds. Can. J. For. Res. 14, 233–237.
Shalaby, A., Tateishi, R., 2007. Remote sensing and GIS for mapping and monitoring land cover and land-use changes in the Northwestern coastal zone of Egypt. Appl. Geogr. 27, 28–41.
Shekede, M., Kusangaya, S., Schmidt, K., 2008. Spatio-temporal variations of aquatic weeds abundance and coverage in lake Chivero, Zimbabwe. Physics and chemistry of the earth. Parts A/B/C 33, 714–721.
Sibanda, M., Mutanga, O., Rouget, M., Odindi, J., 2015. Exploring the potential of in situ hyperspectral data and multivariate techniques in discriminating different fertilizer treatments in grasslands. J. Appl. Remote Sens. 9, 096033.
Siciliano, D., Wasson, K., Potts, D.C., Olsen, R.C., 2008. Evaluating hyperspectral

imaging of wetland vegetation as a tool for detecting estuarine nutrient enrichment. Remote Sens. Environ. 112, 4020–4033.
Wilson, J.R., Richardson, D.M., Rouget, M., Procheş, Ş., Amis, M.A., Henderson, L., Thuiller, W., 2007. Residence time and potential range: crucial considerations in modelling plant invasions. Divers. Distrib. 13, 11–22.
Yuan, F., Sawaya, K.E., Loeffelholz, B.C., Bauer, M.E., 2005. Land cover classification and change analysis of the Twin cities (Minnesota) metropolitan area by multitemporal Landsat remote sensing. Remote Sens. Environ. 98, 317–328.
Zheng, D., Rademacher, J., Chen, J., Crow, T., Bresee, M., Le Moine, J., Ryu, S.-R., 2004. Estimating aboveground biomass using Landsat 7 ETM+ data across a managed landscape in northern Wisconsin. USA. Remote Sens. Environ. 93, 402–411.